

Excitation and charge transfer in proton-lithium collisions at 5–15 keV

M. S. Pindzola

Department of Physics, Auburn University, Auburn, Alabama 36849

(Received 5 April 1999)

Excitation and charge-transfer cross sections for collisions of protons with lithium are calculated by direct solution of the time-dependent Schrödinger equation on a three-dimensional Cartesian lattice. For 5–15-keV incident energies the $1s^2$ core of lithium may be treated effectively using a pseudopotential. For a proton incident on lithium, projections of the time-evolved wave function onto the lattice states of lithium yield excitation cross sections for the $\text{Li}(2s) \rightarrow \text{Li}(2p, 3l)$ transitions. For lithium incident on a proton, projections of the time-evolved wave function onto the lattice states of hydrogen yield charge-transfer cross sections for the $\text{Li}(2s) \rightarrow \text{H}(2l, 3l)$ transitions. The $\text{Li}(2s) \rightarrow \text{Li}(2p)$ excitation and $\text{Li}(2s) \rightarrow \text{H}(2s, 2p)$ charge-transfer cross sections are found to be in good agreement with the crossed-beams experimental measurements of Aumayr *et al.* [J. Phys. B **17**, 4185 (1984); **17**, 4201 (1984); **18**, 2493 (1985)]. [S1050-2947(99)09211-2]

PACS number(s): 34.50.Fa

I. INTRODUCTION

Besides bulk heating, the injection of neutral beams of hydrogen and helium atoms into tokamak plasmas has served as a valuable diagnostic of electron densities, impurity ion temperatures, and electric and magnetic fields. Recently [1], fast neutral lithium atoms have been injected into tokamaks to analyze important boundary-layer plasma parameters. The basic atomic processes in the beam-plasma interaction include ion-impact excitation and charge transfer with the neutral lithium atom.

In this paper we calculate excitation and charge-transfer cross sections for collisions of protons with lithium by direct solution of the time-dependent Schrödinger equation (TDSE) on a three-dimensional Cartesian lattice. This powerful and potentially very accurate numerical method was developed a number of years ago [2–5], but only with the recent development of large distributed-memory parallel computers has application to atomic collision physics been made possible [6–9]. For proton-impact energies below 20 keV, the influence of the $1s^2$ core of lithium on excitation and charge-transfer processes is quite small. Thus, we construct a core pseudopotential and only track the time-dependent behavior of the $2s$ valence electron. For a given incident energy and impact parameter, the time-evolved lattice wave function may be projected onto stationary states to yield a variety of inelastic probabilities. We compare the TDSE lattice results for $\text{Li}(2s) \rightarrow \text{Li}(2p, 3l)$ excitation cross sections and $\text{Li}(2s) \rightarrow \text{H}(2l, 3l)$ charge-transfer cross sections with previous basis-set close-coupling calculations [10–12] and the crossed-beams experimental measurements of Aumayr *et al.* [13–15]. In Sec. II we give an outline of the computational methods, cross-section results are presented in Sec. III, and a brief summary is given in Sec. IV.

II. THEORY

For excitation processes we solve the time-dependent Schrödinger equation for a bare ion (Z) projectile colliding with an atomic target with one valence electron (in atomic units):

$$i \frac{\partial \Psi(\vec{r}, t)}{\partial t} = \left(-\frac{1}{2} \nabla^2 + V_{\text{core}}(r) - \frac{Z}{R(t)} \right) \Psi(\vec{r}, t), \quad (1)$$

where for straight-line trajectories,

$$R(t) = \sqrt{(x-b)^2 + [y - (y_0 + vt)]^2 + z^2}, \quad (2)$$

b is the impact parameter, y_0 is the starting position for the projectile, and v is the projectile velocity. For charge-transfer processes we solve the time-dependent Schrödinger equation for a monovalent atomic projectile colliding with a bare ion target:

$$i \frac{\partial \Psi(\vec{r}, t)}{\partial t} = \left(-\frac{1}{2} \nabla^2 - \frac{Z}{r} + V_{\text{core}}(R(t)) \right) \Psi(\vec{r}, t). \quad (3)$$

The use of the target frame for excitation and the projectile frame for charge transfer allows for center-of-box projection for collision probabilities. The choice of an xy scattering plane guarantees that the collision Hamiltonian has reflection symmetry with respect to the $z=0$ plane.

The core potential, $V_{\text{core}}(r)$, is constructed using standard procedures [16]. For example, the Li^+ ground-state Hartree-Fock orbital $P_{1s}(r)$ is used to construct the Hartree-Slater potential

$$V_{\text{HS}}(r) = 2 \int_0^\infty \frac{P_{1s}^2(r') dr'}{\max(r, r')} - \alpha \left(\frac{24 \rho_{1s}(r)}{\pi} \right)^{1/3}, \quad (4)$$

where α is a free parameter, and $\rho(r) = 2P_{1s}^2(r)/4\pi r^2$ is the radial probability density. The radial Schrödinger equation

$$\left(-\frac{1}{2} \frac{\partial^2}{\partial r^2} - \frac{3}{r} + V_{\text{HS}}(r) - \epsilon_{2s} \right) P_{2s}(r) = 0, \quad (5)$$

is then solved for the Li ground-state orbital $P_{2s}(r)$, with α being adjusted so that ϵ_{2s} agrees with the experimental energy. The inner node of the $P_{2s}(r)$ orbital is removed in a

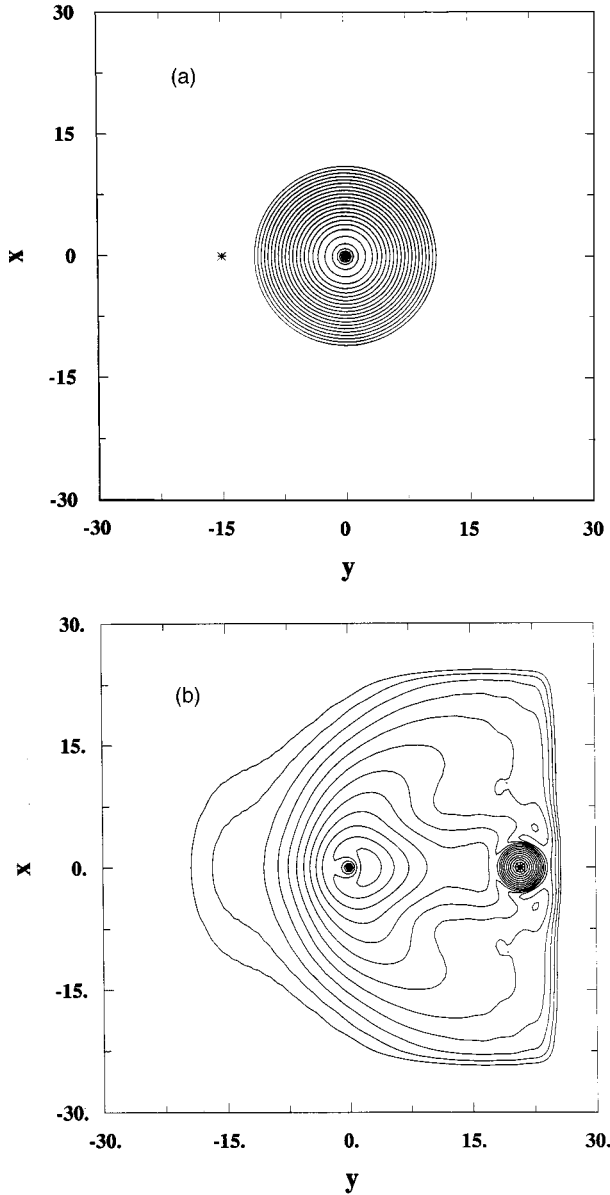


FIG. 1. Time evolution of the electron density in the $z=0$ scattering plane for a proton-lithium collision at 15 keV and zero impact parameter. (a) $t=0.0$, proton at $y=-15.0$; (b) $t=46.0$, proton at $y=+20.8$ (radial distances are in atomic units, $1.0 \text{ a.u.}=5.29 \times 10^{-9} \text{ cm}$).

smooth manner to construct a $P_{2s}(r)$ pseudo-orbital. The core pseudopotential is obtained by inverting the radial Schrödinger equation

$$\left(-\frac{1}{2} \frac{\partial^2}{\partial r^2} + V_{core}(r) - \epsilon_{2s} \right) P_{2s}(r) = 0. \quad (6)$$

The core pseudopotential is strongly repulsive for radial distances less than the inner node of the original $P_{2s}(r)$ orbital.

The stationary states for the monovalent atom are found by relaxation of the time-dependent Schrödinger equation in imaginary time ($\tau = it$):

$$-\frac{\partial \psi_{nlm}^A(\vec{r})}{\partial \tau} = \left(-\frac{1}{2} \nabla^2 + V_{core}(r) \right) \psi_{nlm}^A(\vec{r}), \quad (7)$$

TABLE I. Single-particle energies for the lattice stationary states of lithium and hydrogen.

State	TDSE energy (eV)	Experimental energy (eV)
Li(2s)	-5.38	-5.39
Li(2p)	-3.12	-3.54
Li(3s)	-2.01	-2.02
Li(3p)	-1.41	-1.56
Li(3d)	-1.51	-1.51
H(1s)	-13.47	-13.61
H(2s)	-3.39	-3.40
H(2p)	-3.41	-3.40
H(3s)	-1.51	-1.51
H(3p)	-1.51	-1.51
H(3d)	-1.51	-1.51

while the stationary states for the hydrogenic ion are found by relaxation of

$$-\frac{\partial \psi_{nlm}^I(\vec{r})}{\partial \tau} = \left(-\frac{1}{2} \nabla^2 - \frac{Z}{r} \right) \psi_{nlm}^I(\vec{r}). \quad (8)$$

The relaxed spectrum for the atom and ion incorporates effects due to finite grid spacing and size of the lattice. The excitation probability for the transition $nlm \rightarrow n'l'm'$ at a specific energy and impact parameter is given by

$$\wp_{n'l'm'}(\mathbf{v}, b) = \left| \int d\vec{r} \psi_{n'l'm'}^{A*}(\vec{r}) \Psi(\vec{r}, T) \right|^2, \quad (9)$$

where

$$\Psi(\vec{r}, 0) = \psi_{nlm}^A(x, y, z), \quad (10)$$

and $\Psi(\vec{r}, T)$ is the solution of Eq. (1) at a time T following the collision. The charge-transfer probability for the transition $nlm \rightarrow n'l'm'$ at a specific energy and impact parameter is given by

$$\wp_{n'l'm'}(\mathbf{v}, b) = \left| \int d\vec{r} \psi_{n'l'm'}^{I*}(\vec{r}) \Psi(\vec{r}, T) \right|^2, \quad (11)$$

where

$$\Psi(\vec{r}, 0) = \psi_{nlm}^A(x-b, y-y_0, z) e^{i\mathbf{v}\cdot\mathbf{y}}, \quad (12)$$

TABLE II. Li(2s) \rightarrow Li(2p) excitation cross sections (10^{-15} cm^2).

Final state	Energy (keV)	TDSE	AOCC [12]	Experiment [13]
Li(2p)	5.0	2.28	3.89 ^a	3.19 \pm 0.32
	10.0	3.47	4.28	3.87 \pm 0.39
	15.0	3.49	4.11	3.97 \pm 0.40

^aInterpolated between values at 4.0 and 6.0 keV.

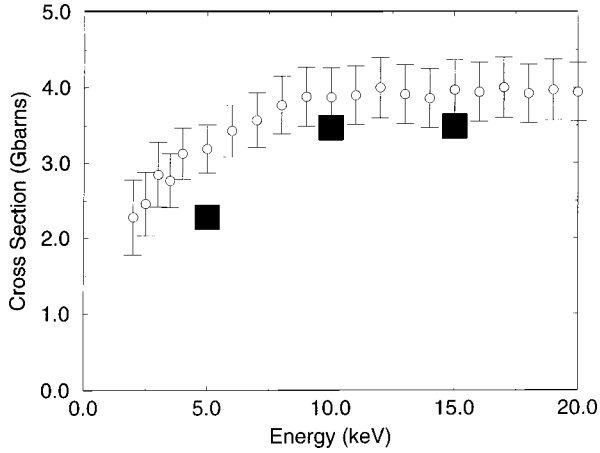


FIG. 2. Excitation cross section for $\text{Li}(2s) \rightarrow \text{Li}(2p)$ vs proton impact energy ($\text{Gbarn} = 1.0 \times 10^{-15} \text{ cm}^2$). Solid square, TDSE calculation; open circles, experiment [13].

and $\Psi(\vec{r}, T)$ is the solution of Eq. (3) at a time T following the collision. The total cross section for either excitation or charge transfer is given by

$$\sigma_{n'l'm'}(\nu) = 2\pi \int_0^\infty \phi_{n'l'm'}(\nu, b) b db. \quad (13)$$

Due to the reflection symmetry with respect to the $z=0$ plane, we need only consider final states with the same $(-1)^{l+m}$ reflection number as the initial state (e.g., even reflection number for the $\text{Li } 2s$ state) [8].

III. RESULTS

Excitation and charge-transfer cross sections for collisions of protons with lithium are calculated by direct solution of Eqs. (1) and (3) on a three-dimensional Cartesian lattice. We employ a $300 \times 300 \times 150$ point lattice with a uniform grid spacing of $\Delta x = \Delta y = \Delta z = 0.2$, yielding a box size of $-30.0 \rightarrow +30.0, -30.0 \rightarrow +30.0, 0.0 \rightarrow +30.0$. We note that radial distances are in atomic units, $1.0 \text{ a.u.} = 5.29 \times 10^{-9} \text{ cm}$. The kinetic energy is represented by three-point central

TABLE III. $\text{Li}(2s) \rightarrow \text{Li}(3l)$ excitation cross sections (10^{-16} cm^2).

Final state	Energy (keV)	TDSE
Li(3s)	5.0	0.99
	10.0	0.28
	15.0	0.53
Li(3p)	5.0	1.03
	10.0	1.26
	15.0	1.43
Li(3d)	5.0	2.49
	10.0	4.89
	15.0	4.21

TABLE IV. $\text{Li}(2s) \rightarrow \text{H}(2l)$ charge-transfer cross sections (10^{-15} cm^2).

Final state	Energy (keV)	TDSE	AOCC [10]	Experiment [14,15]
H(2s)	5.0	1.71	1.51 ^a	2.10 ± 0.71
	10.0	0.59	0.63	0.80 ± 0.26
	15.0	0.20	0.23	0.27 ± 0.11
H(2p)	5.0	3.15	2.56 ^a	2.79 ± 0.89
	10.0	0.98	1.07	1.16 ± 0.37
	15.0	0.27	0.30	0.25 ± 0.10

^aInterpolated between values at 4.0 and 6.0 keV.

differences in each spatial coordinate, while an explicit second-order difference algorithm is used to propagate the solution in time [17]. Spurious wave reflection at the lattice boundary is eliminated through the use of exponential masking.

Solving Eq. (1) we present probability density plots in the $z=0$ scattering plane as a function of time in Fig. 1 for a proton-lithium collision at 15 keV and zero impact parameter. The initial position of the proton is at $\vec{r} = (0.0, -15.0, 0.0)$. For the time frame seen in Fig. 1(b) the proton has moved to $\vec{r} = (0.0, +20.8, 0.0)$ with a sizable ‘‘capture’’ of probability density. Notice the effective suppression of wave reflection at the lattice boundary. Thus, only the time-evolved wave function at the center of the box remains faithful, and only it can be safely projected onto centered stationary states of lithium for the extraction of excitation probabilities. Solving Eq. (3) the time evolution of the probability density for a lithium-proton collision at 15 keV and zero impact parameter is the mirror image of Fig. 1, at least away from the lattice boundary. Again only the time-evolved wave function at the center of the box remains faithful, and only it can be safely projected onto centered stationary states of hydrogen for the extraction of charge-transfer probabilities.

The relatively small size of the lattice means that only the K -, L -, and M -shell stationary states of lithium and hydrogen are well represented. The lattice stationary states of lithium and hydrogen are calculated using Eqs. (7) and (8), and their

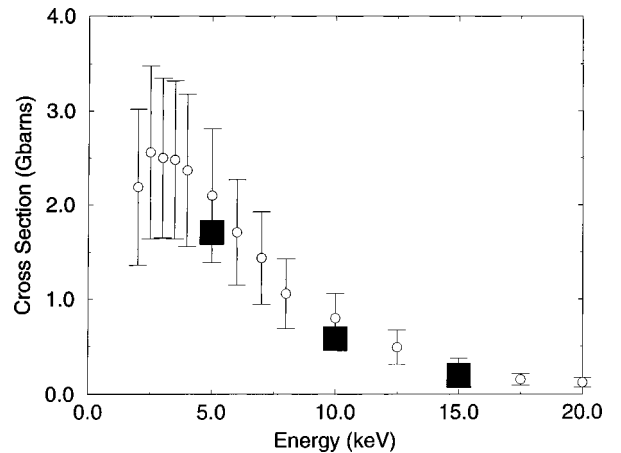


FIG. 3. Charge-transfer cross section for $\text{Li}(2s) \rightarrow \text{H}(2s)$ vs proton impact energy ($\text{Gbarn} = 1.0 \times 10^{-15} \text{ cm}^2$). Solid square, TDSE calculation; open circles, experiment [15].

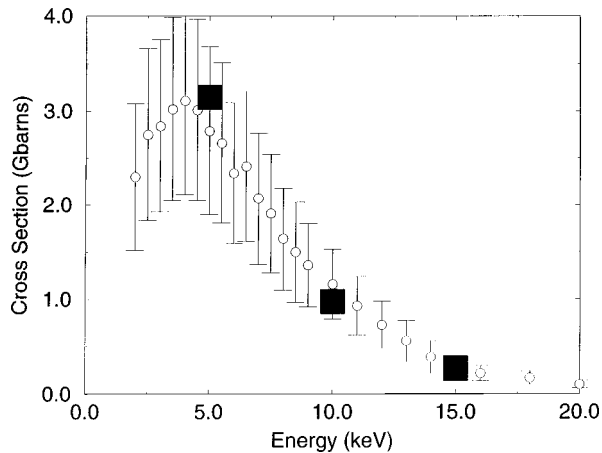


FIG. 4. Charge-transfer cross section for $\text{Li}(2s) \rightarrow \text{H}(2p)$ vs proton impact energy ($\text{Gbarn} = 1.0 \times 10^{-15} \text{ cm}^2$). Solid square, TDSE calculation; open circles, experiment [14].

single-particle energies are compared with experimental values [18] in Table I. The largest difference between theoretical and experimental energies is for the $\text{Li}(np)$ states. A core pseudopotential $V_{\text{core}}(r)$, requiring no explicit l dependence, which will yield both an accurate $2s$ ionization potential and an accurate $2s \rightarrow 2p$ energy splitting, proved difficult to construct.

The excitation probabilities of Eq. (9) are calculated at incident proton energies of 5, 10, and 15 keV and at impact parameters ranging from 0.0 to 20.0. The general shape of an excitation probability as a function of impact parameter varies widely from one transition to the next. For example, the $\text{Li}(2s) \rightarrow \text{Li}(2p)$ excitation probability at $E = 5.0$ keV has a large almost symmetrical peak centered at $b = 7.0$, moving to slightly lower impact parameters as the incident energy is increased. On the other hand, the $\text{Li}(2s) \rightarrow \text{Li}(3s)$ excitation probability at $E = 5.0$ keV has a peak at $b = 0.0$ and a second larger peak at $b = 6.0$. As the incident energy is increased the zero impact parameter peak grows and the second peak almost vanishes by $E = 15.0$ keV. The charge-transfer probabilities of Eq. (11) are calculated at incident proton energies of 5, 10, and 15 keV and at impact parameters ranging from 0.0 to 14.0. The $\text{Li}(2s) \rightarrow \text{H}(2p)$ charge-transfer probability at $E = 5.0$ keV has a large double humped central peak at $b = 5.0$, which coalesces and then moves to smaller impact parameters as the incident energy increases.

Excitation cross sections for the $\text{Li}(2s) \rightarrow \text{Li}(2p)$ transition are presented in Table II and Fig. 2 at incident proton energies of 5, 10, and 15 keV. The TDSE lattice results and recent atomic-orbital close-coupling (AOCC) calculations [12] bracket the crossed-beams experimental measurements of Aumayr *et al.* [13]. Additional excitation cross sections for the $\text{Li}(2s) \rightarrow \text{Li}(3l)$ transitions are presented in Table III. Charge-transfer cross sections for the $\text{Li}(2s) \rightarrow \text{H}(2l)$ transitions are presented in Table IV and Figs. 3 and 4 at incident proton energies of 5, 10, and 15 keV. The TDSE lattice results and the AOCC calculations of Fritsch and Lin [10] are both within the absolute error bars of the crossed-beams experimental measurements of Aumayr *et al.* [14,15]. Additional charge-transfer cross sections for the $\text{Li}(2s) \rightarrow \text{H}(3l)$ transitions are presented in Table V; and are found to be in

TABLE V. $\text{Li}(2s) \rightarrow \text{H}(3l)$ charge-transfer cross sections (10^{-16} cm^2).

Final state	Energy (keV)	TDSE	AOCC [10]	Experiment [14]
$\text{H}(3s)$	5.0	1.61	1.00 ^a	2.03 ± 1.02^b
	10.0	2.18	1.70	3.35 ± 1.68^b
	15.0	0.89	1.30	1.99 ± 1.00^b
$\text{H}(3p)$	5.0	3.12	1.90 ^a	3.05 ± 1.68^c
	10.0	2.23	1.80	2.56 ± 1.41^c
	15.0	0.88	1.40	1.33 ± 0.73^c
$\text{H}(3d)$	5.0	2.13	1.80 ^a	1.01 ± 0.51^b
	10.0	0.50	0.60	0.37 ± 0.19^b
	15.0	0.16	0.30	0.28 ± 0.14^b

^aInterpolated between values at 4.0 and 6.0 keV.

^b H_α emission.

^c L_β emission.

reasonable agreement with AOCC calculations [10] and experimental measurements [14].

IV. SUMMARY

Inelastic cross sections for proton-lithium collisions are calculated by direct solution of the time-dependent Schrödinger equation on a three-dimensional Cartesian lattice. The use of a large number of lattice points ensures a faithful representation of continuum processes, in general superior to most finite basis-set expansions. A pseudopotential is introduced to represent the lithium atomic core. Thus, in principle, the TDSE lattice method may be applied to a bare ion of arbitrary charge colliding with any monovalent atom. In practice, the use of a core pseudopotential restricts the application of the method to an impact energy range in which the core electrons have negligible influence on inelastic processes. For proton-lithium collisions, the TDSE lattice results in the intermediate energy range less than 20 keV, for both the $\text{Li}(2s) \rightarrow \text{Li}(2p)$ excitation and the $\text{Li}(2s) \rightarrow \text{H}(2l)$ charge transfer, are in good agreement with previous basis-set close-coupling calculations and crossed-beams experimental measurements. In the future we plan to extend the TDSE lattice method to investigate ion-atom collisions in external fields, reduced symmetry problems being ideal for a computational method already formulated in a full three-dimensional space.

ACKNOWLEDGMENTS

I would like to thank Dr. Dario Mitnik and Dr. David R. Schultz for useful comments on the manuscript. This work was supported in part by the U.S. Department of Energy under Grant No. DE-FG05-96-ER54348 with Auburn University. Computational work was carried out at the National Energy Research Supercomputer Center in Berkeley, CA.

- [1] R. P. Schorn, E. Wolfrum, F. Aumayr, E. Hintz, D. Rusbuldt, and H. Winter, *Nucl. Fusion* **32**, 351 (1992).
- [2] V. Maruhn-Rezwani, N. Grün, and W. Scheid, *Phys. Rev. Lett.* **43**, 512 (1979).
- [3] C. Bottcher, *Phys. Rev. Lett.* **48**, 85 (1982).
- [4] K. C. Kulander, K. R. Sandhya Devi, and S. E. Koonin, *Phys. Rev. A* **25**, 2968 (1982).
- [5] J. D. Garcia, *Nucl. Instrum. Methods Phys. Res. A* **240**, 552 (1985).
- [6] D. R. Schultz, P. S. Krstic, C. O. Reinhold, and J. C. Wells, *Phys. Rev. Lett.* **76**, 2882 (1996).
- [7] J. C. Wells, D. R. Schultz, P. Gavras, and M. S. Pindzola, *Phys. Rev. A* **54**, 593 (1996).
- [8] A. Kolakowska, M. S. Pindzola, F. Robicheaux, D. R. Schultz, and J. C. Wells, *Phys. Rev. A* **58**, 2872 (1998).
- [9] A. Kolakowska, M. S. Pindzola, and D. R. Schultz, *Phys. Rev. A* **59**, 3588 (1999).
- [10] W. Fritsch and C. D. Lin, *J. Phys. B* **16**, 1595 (1983).
- [11] A. M. Ermolaev, *J. Phys. B* **17**, 1069 (1984).
- [12] R. Brandenburg, J. Schweinzer, F. Aumayr, and H. P. Winter, *J. Phys. B* **31**, 2585 (1998).
- [13] F. Aumayr, M. Fehringer, and H. Winter, *J. Phys. B* **17**, 4185 (1984).
- [14] F. Aumayr, M. Fehringer, and H. Winter, *J. Phys. B* **17**, 4201 (1984).
- [15] F. Aumayr, G. Lakits, W. Hisinsky, and H. Winter, *J. Phys. B* **18**, 2493 (1985).
- [16] P. A. Christiansen, Y. S. Lee, and K. S. Pitzer, *J. Chem. Phys.* **71**, 4445 (1979).
- [17] W. H. Press, S. A. Teukolsky, W. T. Vetterling, and B. P. Flannery, *Numerical Recipes* (Cambridge Press, Cambridge, England, 1992), p. 833.
- [18] C. E. Moore, *Atomic Energy Levels*, Natl. Bur. Stand. Ref. Data Ser., Natl. Bur. Stand. (U.S.) Circ. No. 35 (U.S. GPO, Washington, DC, 1971), Vol. I.